Pergamon

Geochimica et Cosmochimica Acta, Vol. 66, No. 9, pp. 1641–1650, 2002

0016-7037/02 $22.00 + .00

PII S0016-7037(01)00866-3

Ba diffusion in feldspar

D. J. CHERNIAK

Department of Earth and Environmental Sciences, Rensselaer Polytechnic Institute, Troy, NY 12180, USA

(*Received June* 28, 2001; *accepted in revised form November* 14, 2001)

Abstract—Diffusion of Ba in natural sanidine and plagioclase has been characterized under dry 1 atm conditions. Polished or cleaved sections of the feldspars were surrounded by source powders in Pt capsules and annealed in air. Sources of diffusant consisted of BaO, SiO_2 and Al_2O_3 powders mixed with ground feldspar and prereacted in Pt crucibles at 975°C. Prepared sample capsules were annealed for times ranging from 1 h to a few months at temperatures from 775 to 1124°C. The Ba distributions in the feldspars were profiled by Rutherford Backscattering Spectrometry (RBS).

The following Arrhenius relation is obtained for Ba diffusion in sanidine (Or_{61}) for diffusion normal to the (001) cleavage face:

$$D_{san} = 2.9 \times 10^{-1} \exp(-455 \pm 20 \text{ kJ mol}^{-1}/RT) \text{ m}^2\text{sec}^{-1}.$$

Diffusion normal to (010) appears to be slightly slower than diffusion normal to (001).

For diffusion normal to (001) and normal to (010) in labradorite (An_{67}), the Arrhenius relations are, respectively,

$$D_{lab\perp(001)} = 2.3 \times 10^{-7} \exp(-323 \pm 20 \text{ kJ mol}^{-1}/RT) \text{ m}^2\text{sec}^{-1}$$

$$D_{lab\perp(010)} = 1.1 \times 10^{-6} \exp(-341 \pm 23 \text{ kJ mol}^{-1}/RT) \text{ m}^2\text{sec}^{-1}$$

Diffusion in oligoclase (An_{23}) can be described by the following Arrhenius relations:

$$D_{olig\perp(001)} = 1.7 \times 10^{-7} \exp(-303 \pm 32 \text{ kJ mol}^{-1}/RT) \text{ m}^2\text{sec}^{-1}$$

$$D_{olig\perp(010)} = 1.1 \times 10^{-4} \exp(-377 \pm 28 \text{ kJ mol}^{-1}/RT) \text{ m}^2\text{sec}^{-1}$$

Ba diffusion in sanidine is more than an order of magnitude slower than Sr diffusion measured on specimens of the same composition (Cherniak, 1996), a not unexpected result given the significantly larger ionic radius of Ba. Similarly, in both of the plagioclase compositions, Ba diffusion is slower than Sr or Pb diffusion by about two orders of magnitude.

These slower diffusivities indicate that Ba zoning will be preserved under more extreme thermal conditions than those under which Sr zoning is retained. For example, at 700°C, zones on the scale of 100-μm width will retain Ba chemical signatures for times $>$ 10 Ma. Sr zoning in regions of comparable width will be preserved for time periods approximately an order of magnitude shorter at this temperature.

1. INTRODUCTION

The process of diffusion plays a significant role in the distribution of trace elements and isotopes within and among minerals in rocks exposed to elevated temperatures for extended periods of time. In previous work on the feldspars, we have measured Sr (Cherniak and Watson, 1992, 1994; Cherniak, 1996) and Pb diffusion (Cherniak, 1995) in specimens of plagioclase and alkali feldspars over a range of compositions, which has contributed to understanding the importance of diffusion in influencing measured Sr and Pb isotopes and chemical signatures of these elements. In this study, we investigate the diffusion of Ba in plagioclase and alkali feldspars.

Whereas Ba is most often found at trace or minor levels in feldspars (typically 10^3–10^4 ppm for alkali feldspars, a few to several thousand ppm for plagioclase; Smith and Brown, 1988), some feldspars, especially potassium feldspars, can have high percentages of celsian ($BaAl_2Si_2O_8$) component. Hyalophane ($(K,Na,Ba)[(Al,Si)_4O_8]$) can have 5 to 30% of the celsian molecule incorporated (Deer et al., 1992). Plagioclase feldspars bearing barium are less common, but barium-oligoclase, barium-bytownite, and barium anorthite (calciocelsian) are known. Zoning of trace and minor elements (including Ba) in plagioclase and sanidine phenocrysts provide insight into chemical and physical evolution of magma chambers (e.g., Singer et al., 1995; Anderson et al., 2000), and trace element concentrations in cores of anorthitic megacrysts can offer a means to sample earlier stages of magmatic evolution before fractional crystallization and magma mixing (e.g., Bindeman and Bailey, 1999).

Like the cations Sr and Pb, for which we have, as noted above, already investigated diffusion in feldspars, Ba is divalent. However, the significantly larger size of Ba compared with these cations permits us to investigate the influence of cation size on diffusion rates in feldspars and consider whether these trends mirror those observed for univalent cations in plagioclase (Giletti and Shanahan, 1997).

* Author to whom correspondence should be addressed (chernd@rpi.edu).

2. MATERIAL AND METHODS

Ba diffusion coefficients were determined in three natural feldspars of differing composition. The feldspars used in this study were a sanidine (Or_{61}) from Sri Lanka, an oligoclase (An_{23}) from North Carolina, both kindly provided by Don Miller, and a labradorite (An_{67}) from Lake County, Oregon, obtained from the collection at the National Museum of Natural History (NMNH # 135512-1). We have previously measured Sr diffusion in all three of these feldspars (Cherniak and Watson, 1994; Cherniak, 1996) and Pb diffusion in the plagioclase (Cherniak, 1995). Compositional analyses of the sanidine and plagioclase are presented in Cherniak and Watson (1994) and Cherniak (1996), respectively.

Natural cleavage faces were used in experiments on all feldspars in measurements of diffusion normal to (001) and for diffusion normal to (010) in sanidine. For diffusion normal to (010) in the two plagioclase compositions, samples were sectioned with a low-speed saw and polished to 0.05-μm gamma alumina. All samples were cleaned ultrasonically in distilled water and ethanol and cut into pieces of surface area 10 to 20 mm^2. Both polished and cleaved samples were then annealed in air at 1000°C for 48 h. This preannealing step serves to remove possible surface damage produced by cold working the polished samples and to equilibrate point defects of all samples to conditions that would be similar to those experienced during the experiments. This annealing step may also induce in the feldspars a similar state of Al-Si disorder (e.g., Smith and Brown, 1988; Griffen; 1992); however, the duration of the anneals may not be sufficient to allow for complete disordering if this process occurs solely by Al-Si diffusive exchange, which is likely the case for 1-atm anhydrous conditions (e.g., Sipling and Yund, 1974; Grove et al., 1984; Goldsmith and Jenkins, 1985). Evidence from the literature (e.g., Smith and Brown, 1988; Behrens et al., 1990) suggests that plagioclase of similar compositions from the same localities as those used in the present study may be in an intermediate state of order. Although we cannot precisely characterize the state of Al-Si order in each feldspar before and after annealing, this is not necessarily a factor that will significantly influence results; some studies suggest that the degree of Al-Si order will not greatly affect diffusivities (e.g., Yund, 1983). In addition, measurements on plagioclases of similar composition but from different localities (and presumably in somewhat different states of Al-Si order and with differing defect concentrations and microstructural states) yield similar diffusivities for divalent cations (e.g., Behrens et al., 1990; Cherniak and Watson, 1992, 1994; Giletti and Casserly, 1994).

The sources of Ba for the experiments were mixtures of BaO, Al_2O_3, and SiO_2 powders and finely ground feldspar (of the same composition as the samples) in 3 : 1 (by weight) ratio. The oxide powders, in weight ratio of 1.5 : 1 : 1.2 for BaO : Al_2O_3 : SiO_2 were mixed thoroughly under alcohol and dried. The oxide powder mixture was then combined with the ground feldspar, and the mixture heated in a Pt crucible at 970°C for ~2 d. The source material was then reground before use. Experiments were assembled by placing the source mixture and feldspar specimen in a 5-mm Pt capsule. After loading, the Pt capsule was crimped shut.

Prepared sample capsules were annealed in 1-atm furnaces at temperatures from 775 to 1124°C for times ranging from 1 h to 3 months. A "zero-time" experiment was also run at 950°C for the sanidine. For this experiment, the sample capsule was prepared as above; the sample was placed in the furnace, brought up to run temperature, and immediately quenched. Temperatures in the 775 to 1075°C experiments were monitored with type K (chromel-alumel) thermocouples during the course of the anneals; temperature uncertainties were ± 2°C. A type S (Pt-Pt 10% Rh) thermocouple was used for the higher-temperature run, with comparable temperature uncertainty. On completion of the anneals, samples were quenched merely by removing them from furnaces and permitting them to cool in air. Samples were then removed from capsules, freed of residual source material, and cleaned ultrasonically in successive baths of distilled water and ethanol. The samples were readily removed from the source material, and sample surfaces using these sources were easily cleaned of the residual, as was the case for similar sources used in our Sr diffusion studies (Cherniak and Watson, 1992, 1994; Cherniak, 1996).

2.1. RBS Analysis

RBS has been used in our measurements of Pb and Sr diffusion in feldspars (Cherniak and Watson, 1992, 1994; Cherniak, 1995, 1996) and in many other diffusion studies. The experimental and analytical approach used here is similar to that used in our previous work. Helium beam energies used ranged between 1 and 2 MeV, with incident energies in the lower range used in some analyses to improve sensitivity. Spectra were converted to Ba concentration profiles employing procedures outlined in publications cited above. The data processing routine used to extract depth scales from the raw data took into account the compositional differences of the feldspars employed in this study and the effect of this variation on stopping powers for the helium ions. The resultant profiles (concentration vs. depth) were fit with a solution to Fick's Second Law involving one-dimensional, concentration-independent diffusion in a semi-infinite medium with a source reservoir maintained at constant concentration (i.e., a complementary error function solution). Diffusion coefficients were evaluated by plotting the inverse of the error function, i.e., $erf^{-1}((C_o - C(x,t))/C_o)$ vs. depth (x), in the sample. A straight line of slope $(4Dt)^{-1/2}$ results if the data satisfy the conditions of the model. C_o, the surface concentration of diffusant, is determined by iteratively varying its value until the intercept of the line converges on zero. In Figure 1, typical diffusion profiles and their inversions through the error function are shown. The uncertainties in concentration and depth from each data point (mainly derived from counting statistics in the former and detector resolution in the latter) were used to evaluate the uncertainties in the diffusivities determined from the fits to the model. The profiles produced in the diffusion anneals agree quite well with the curves for the chosen solution to Fick's Second Law, confirming its appropriateness in describing diffusion given the initial and boundary conditions imposed in the experiments.

3. RESULTS

The results for Ba diffusion anneals with the sanidine are presented in Table 1 and plotted in Figure 2. For diffusion normal to (001), an activation energy, 455 ± 20 kJ mol^{-1} (108.5 ± 4.8 kcal mol^{-1}), and preexponential factor, 2.9 × 10^{-1} m^2sec^{-1} (log D_o = −0.540 ± 0.841), are obtained. Diffusion coefficients for the direction normal to (010) are comparable to those for transport normal to (001), a finding similar to that for Sr diffusion in sanidine (Cherniak, 1996).

The results for experiments on the oligoclase are presented in Table 1 and plotted in Figure 3. For transport normal to (001), the activation energy is 303 ± 32 kJ mol^{-1} (72.5 ± 7.6 kcal mol^{-1}); the preexponential factor is 1.73 × 10^{-7} m^2sec^{-1} (log D_o = −6.76 ± 1.40). The activation energy for diffusion normal to (010) is considerably larger, with a value of 377 ± 28 kJ mol^{-1} (90.0 ± 6.7 kcal mol^{-1}); the preexponential factor is 1.09 × 10^{-4} m^2sec^{-1} (log D_o = −3.96 ± 1.14). Anisotropy of diffusion in oligoclase, with diffusion normal to (010) the slower, has also been observed for Pb diffusion (Cherniak, 1995).

Results for diffusion measurements on the labradorite are plotted in Figure 4 and presented in Table 3. An activation energy of 323 ± 20 kJ mol^{-1} (77.2 ± 4.8 kcal mol^{-1}), and preexponential factor of 2.25 × 10^{-7} m^2sec^{-1} (log D_o = −6.65 ± 0.84) are determined for transport normal to (001). Diffusion normal to (010) proceeds at a similar rate, with activation energy of 341 ± 23 kJ mol^{-1} (81.5 ± 5.5 kcal mol^{-1}) and preexponential factor of 1.05 × 10^{-6} m^2sec^{-1} (log D_o = −5.98 ± 0.99).

As earlier noted, we performed zero-time experiments on the sanidine, as well as a time-series study at 975°C, to verify that the measured concentration profiles represent volume diffusion and are not a result of other phenomena such as surface reaction that may otherwise result in enhanced Ba yields in the near-surface region. The zero-time anneal also serves to highlight possible systematic problems in the experimental approach. In Figure 5, the results from the time series at 975°C are plotted. Diffusivities at

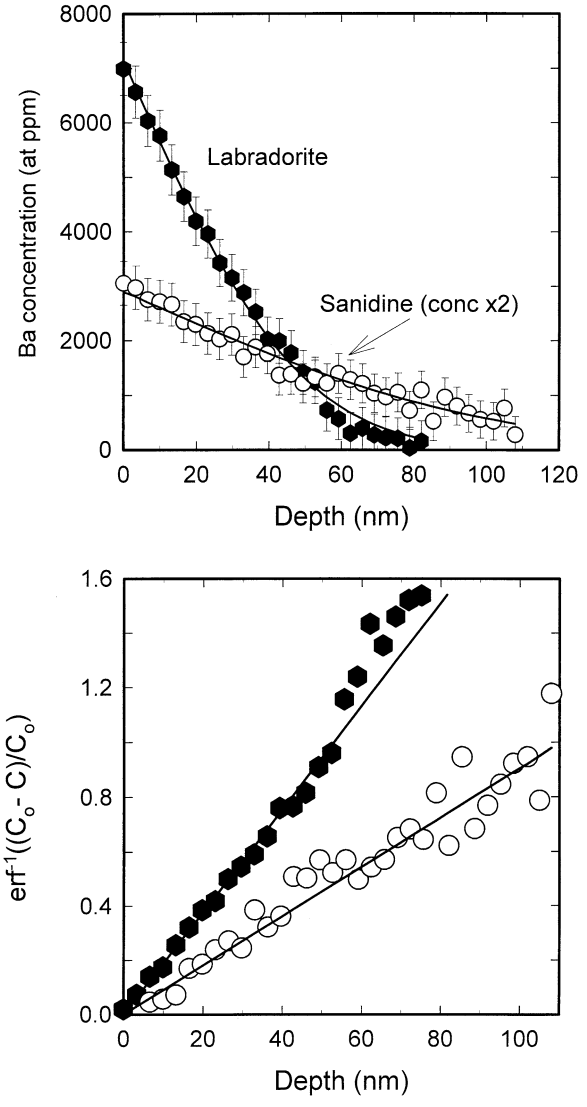

Fig. 1. Typical Ba diffusion profiles for experiments on labradorite and sanidine. (a) The measured diffusion profiles are plotted with complementary error function curves. (b) The data are linearized by inversion through the error function. Slopes of the lines are equal to $(4Dt)^{-1/2}$. The labradorite sample was annealed for 7.5 h at 1027°C and the sanidine for 46 h at 974°C.

this temperature are quite similar for times ranging over more than an order of magnitude, suggesting that volume diffusion is the dominant contributor to the observed diffusion profiles. The zero-time experiment (not shown) displays little evidence of significant uptake of Ba in the near-surface region during the heatup and quench phases of the anneal, offering further confirmation that Ba profiles are a consequence primarily of lattice diffusion.

4. DISCUSSION

4.1. Effect of Feldspar Composition on Diffusion Coefficients

Arrhenius relations for Ba diffusion in the investigated feldspar compositions are shown in Figure 6. Although only two plagioclase compositions were used in experiments, the data indicate that diffusion coefficients are higher for more sodic plagioclase, a finding consistent with observations for Sr (Cherniak and Watson, 1994; Giletti and Casserly, 1994) and Pb (Cherniak, 1995). For diffusion normal to (001), Ba diffusion in oligoclase is about an order of magnitude faster than in labradorite, whereas activation energies for diffusion are comparable.

Diffusivities in the plagioclase and sanidine do not differ by much more than an order of magnitude over the temperature range of our experiments; at lower temperatures, however, variances among these feldspars can be quite pronounced because of the significantly higher activation energy for diffusion in sanidine. For example, at 500°C, Ba diffusion in sanidine will be from two to four orders of magnitude smaller than in the plagioclase compositions studied here. It is important, however, to note that such comparisons apply strictly to structurally and compositionally homogeneous feldspars. Exsolution may be a significant consideration in natural systems. Since exsolution in alkali feldspars is rate-limited by alkali diffusion, it will proceed much more rapidly than Ba diffusion and faster than unmixing of intermediate plagioclase. Given the complexity of these processes, however, it is difficult to make general statements about the behavior and redistribution of Ba during exsolution.

4.2. Comparison with Diffusion Coefficients for Other Cations in Feldspar

Plots of diffusion data for various cations in the feldspar compositions investigated in this study are presented in Figure 7. Diffusion of several other divalent cations has been measured in labradorite (Fig. 7a). Behrens et al. (1990) have measured Ca diffusion using a ^{45}Ca tracer, whereas Cherniak and Watson (1994) and Cherniak (1995) have measured Sr and Pb diffusion, respectively, in labradorite from the same locality. Ca diffusion is about two orders of magnitude faster than Ba diffusion, although the activation energy for Ca diffusion (311 ± 11 kJ mol^{-1}) is similar to values measured for Ba diffusion. Ba diffusion is likely slowed by its relatively large ionic radius (1.35 Å for Ba vs. 1.00 Å for Ca [Shannon, 1976] in sixfold coordination [Smyth and Bish, 1988]), although both may move by similar mechanisms. Diffusion of Sr and Pb are also faster than Ba, and they diffuse slightly more slowly than Ca, a reasonable finding given their intermediate ionic radii (1.18 and 1.19 Å for Sr and Pb, respectively). However, both Pb and Sr diffusion exhibit some anisotropy, with diffusion normal to (001) faster than diffusion normal to (010) by ~0.7 log unit; similar anisotropy is not evident for Ba. The reason for this difference is unclear. Activation energies for Ba diffusion are somewhat larger (323 and 341 kJ mol^{-1}) than those for either Sr (268 kJ mol^{-1}) or Pb (267 kJ mol^{-1}).

The dependence of diffusion rate on size has been shown for univalent cations in labradorite (Giletti and Shanahan, 1997), with Na (1.02 Å) diffusing at a rate two to three orders of magnitude faster than K (1.38 Å); these univalent cations differ in size by an amount comparable to that separating the divalent cations Ba and Ca. Similar trends of increasing D with decreasing ionic radius have been noted in near-endmember plagioclase compositions for both divalent cations in anorthite (La Tourette and Wasserburg, 1998) and univalent cations in albite

Table 1. Ba diffusion in Feldspar.

	T(°C)	time(s)	D(m^2sec^{-1})	log D	±
Sanidine (Or_{61})					
normal to (001):					
SanBa-5	1075	5.40×10^3	6.21×10^{-19}	−18.21	0.10
SanBa-3	1026	2.16×10^4	1.08×10^{-19}	−18.97	0.13
SanBa-4c	976	3.24×10^4	2.61×10^{-20}	−19.58	0.09
SanBa-2	975	2.88×10^4	3.62×10^{-20}	−19.44	0.16
SanBa-7	974	1.66×10^5	1.84×10^{-20}	−19.74	0.11
SanBa-8	974	8.64×10^4	3.03×10^{-20}	−19.52	0.11
SanBa-6	926	5.26×10^5	5.93×10^{-21}	−20.23	0.08
SanBa-10	876	1.56×10^6	3.03×10^{-22}	−21.52	0.16
SanBa-9	828	3.89×10^6	4.54×10^{-23}	−22.34	0.26
normal to (010):					
SanBa-4b	976	3.24×10^4	1.36×10^{-20}	−19.87	0.10
Labradorite (An_{67})					
normal to (001):					
LabBa-4c	1074	5.40×10^3	9.17×10^{-20}	−19.04	0.27
LabBa-3c	1027	2.70×10^4	2.26×10^{-20}	−19.65	0.10
LabBa-2c	972	9.60×10^4	5.33×10^{-21}	−20.27	0.13
LabBa-1c	926	4.32×10^5	2.19×10^{-21}	−20.66	0.07
LabBa-5c	877	1.46×10^6	1.65×10^{-22}	−21.78	0.16
LabBa-7c	821	3.98×10^6	9.44×10^{-23}	−22.03	0.20
LabBa-6c	777	8.09×10^6	2.63×10^{-23}	−22.58	0.19
normal to (010):					
LabBa-9	1124	3.60×10^3	3.08×10^{-19}	−18.51	0.26
LabBa-4b	1074	5.40×10^3	1.21×10^{-19}	−18.92	0.15
LabBa-3b	1027	2.70×10^4	2.60×10^{-20}	−19.59	0.13
LabBa-2b	972	9.60×10^4	3.03×10^{-21}	−20.52	0.13
LabBa-1b	926	4.32×10^5	6.17×10^{-22}	−21.21	0.18
LabBa-5b	877	1.46×10^6	1.90×10^{-22}	−21.72	0.13
LabBa-7b	821	3.98×10^6	6.56×10^{-23}	−22.18	0.17
LabBa-6b	777	8.09×10^6	4.52×10^{-23}	−22.35	0.20
Oligoclase (An_{23})					
normal to (001):					
OligBa-4c	1023	1.98×10^4	1.70×10^{-19}	−18.77	0.24
OligBa-3c	976	8.64×10^4	2.87×10^{-20}	−19.54	0.28
OligBa-1c	927	4.37×10^5	9.39×10^{-21}	−20.03	0.12
OligBa-2c	878	1.30×10^6	2.72×10^{-21}	−20.57	0.34
OligBa-6c	830	4.81×10^6	7.27×10^{-22}	−21.14	0.30
OligBa-7	775	6.68×10^6	1.71×10^{-22}	−21.77	0.25
normal to (010):					
OligBa-5	1072	3.60×10^3	4.89×10^{-19}	−18.31	0.22
OligBa-4b	1023	1.98×10^4	9.63×10^{-20}	−19.02	0.19
OligBa-3b	976	8.64×10^4	1.35×10^{-20}	−19.87	0.11
OligBa-1b	927	4.37×10^5	2.29×10^{-21}	−20.64	0.20
OligBa-2b	878	1.30×10^6	1.17×10^{-21}	−20.93	0.11
OligBa-6b	830	4.81×10^6	1.64×10^{-22}	−21.79	0.28

(Giletti and Shanahan, 1997). It is also evident that diffusion coefficients are significantly influenced by cation charge. Both K and Na diffusion are faster than diffusion of all of the divalent cations, and diffusion of Ba is about three orders of magnitude slower than diffusion of K, which has a comparable ionic radius but lower charge.

In oligoclase, the trends noted for labradorite also broadly apply (Fig. 7b). However, diffusion of Ba and Pb exhibit more marked anisotropy, with diffusion normal to (010) slower than diffusion normal to (001). In both cases, activation energies for diffusion are also larger for transport normal to (010). It may be that the relatively large size of these cations leads to anisotropy in diffusion, since diffusion normal to (010) in the feldspar structure must involve movement through interstitial sites or other high-energy positions, which may be energetically less favorable for large cations. Activation energies for diffusion are somewhat larger for Ba than Pb (303 vs. 261 kJ mol^{-1} and 377 vs. 355 kJ mol^{-1} for diffusion normal to (001) and (010), respectively), but values overlap within experimental uncertainty.

In sanidine (Fig. 7c) Ba also diffuses more slowly, but the difference between Sr and Ba diffusion coefficients is somewhat smaller than in plagioclase. This may be the case because Ba is more readily accommodated in the lattice of potassium-rich feldspars, given the similarities in ionic radius of K and Ba. In addition, charge-compensating species would be necessary to facilitate exchange of divalent cations in alkali feldspars, whereas direct exchange of Ca for divalent diffusing cations can occur in all but the most albitic plagioclase. Movement of charge-compensating species may impose a rate-limiting factor on transport of divalent species in alkali feldspars, thus reducing the dependence of diffusion on ionic radius for like-charged cations. Although tracer diffusion of the alkalis has not been measured in alkali feldspar of this composition, Christofferson

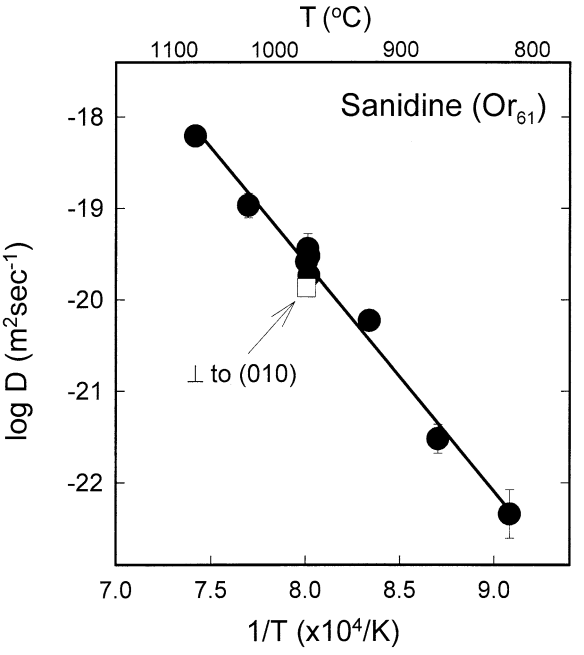

Fig. 2. Arrhenius plot of Ba diffusion results for sanidine. The line is a least-squares fit to the diffusion data for transport normal to (001). For this orientation, an activation energy of 455 kJ mol^{-1} and preexponential factor 2.9×10^{-1} m^2sec^{-1} are obtained. Diffusion normal to (010) is similar in magnitude.

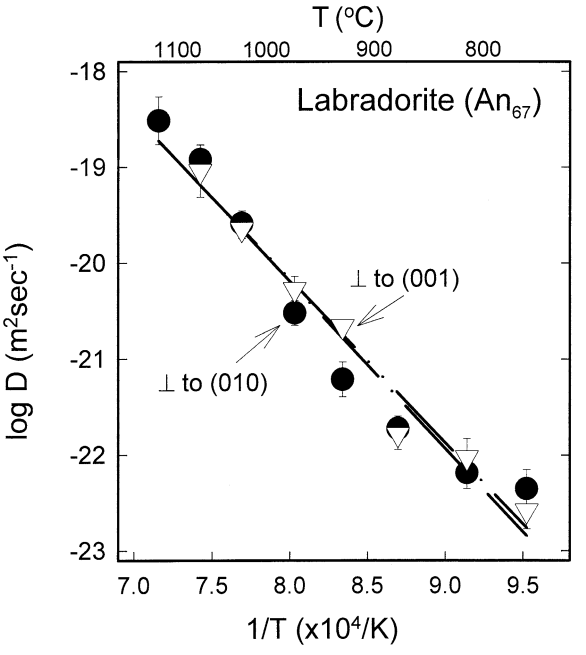

Fig. 4. Arrhenius plot of Ba diffusion data for labradorite. From the least-squares fit to the diffusion data, an activation energy of 323 kJ mol^{-1} and preexponential factor 2.3×10^{-7} m^2sec^{-1} for diffusion normal to (001). Diffusion normal to (010) proceeds at a similar rate.

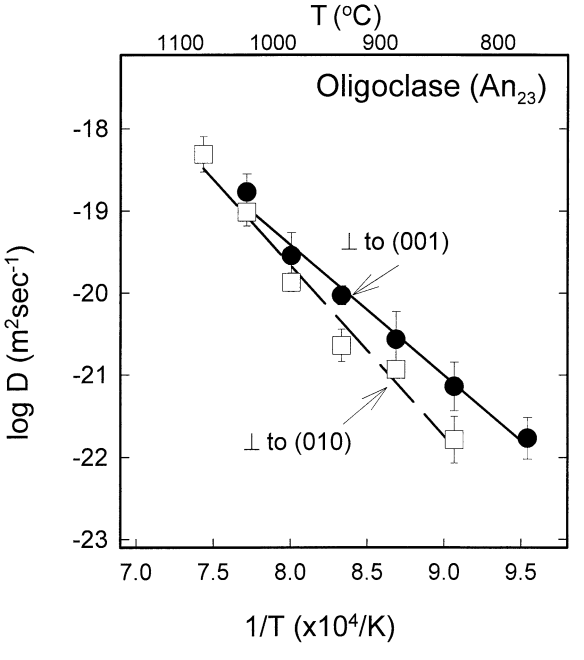

Fig. 3. Arrhenius plot for Ba diffusion in oligoclase. From a fit to the diffusion data, we obtain an activation energy of 303 kJ mol^{-1} and preexponential factor 1.7×10^{-7} m^2sec^{-1} for transport normal to (001). There is some anistropy in Ba diffusion, with the activation energy for transport normal to (010) somewhat higher (377 kJ mol^{-1}) and diffusivities slower.

et al. (1983) have measured K-Na interdiffusion in alkali feldspars. From their data at two different temperatures, we estimate K-Na interdiffusion rates for an alkali feldspar with 61% orthoclase component. As might be expected, alkali interdiffusion is considerably faster than diffusion of either Sr or Ba, differing by two to three orders of magnitude and approximately four orders of magnitude, respectively.

In addition to ion size and charge considerations, the elastic properties of the mineral lattice may also be important influ-

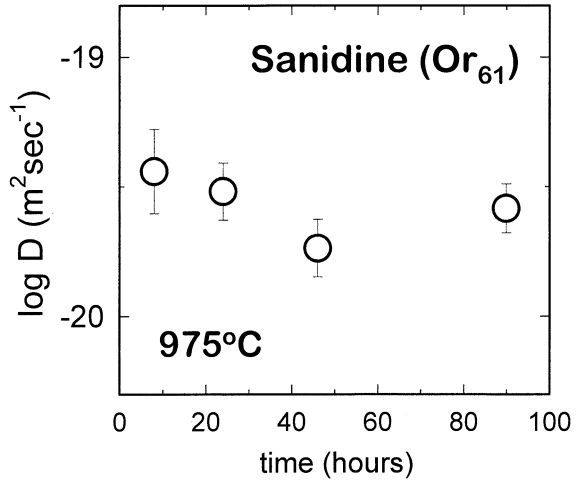

Fig. 5. Time series for Ba diffusion in sanidine, with experiments run at 975°C. Diffusion rates are quite similar, despite differences in anneal times ranging over about an order of magnitude, suggesting that the dominant process being measured is volume diffusion.

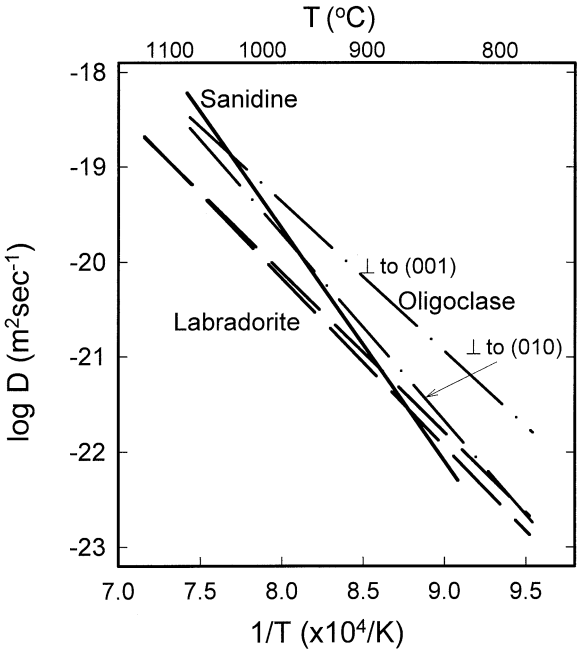

Fig. 6. Summary of Ba diffusion data for feldspar compositions investigated in this work. Among the plagioclases, diffusion is faster for the more sodic oligoclase, especially in the direction normal to (001). Ba diffusivities in sanidine are comparable those in plagioclase in the investigated temperature range, but the activation energy for Ba diffusion in sanidine is significantly higher.

ences on diffusion. Elastic properties have been shown to influence partitioning behavior in plagioclase (Blundy and Wood, 1991), in which the more flexible sodic plagioclase structure accommodates Sr and Ba ions more readily than does the more rigid calcic plagioclase; they have further extended these arguments and developed a predictive model (Blundy and Wood, 1994) to estimate partition coefficients as functions of Young's moduli and cation size and charge. Similar intuitive reasoning can be applied to diffusional behavior if we conjecture that a more flexible (i.e., smaller elastic modulus) structure would also permit easier cation migration, which is consistent with our observations of faster cation diffusivities with increasing Na content of plagioclase.

It should be noted, however, that the Blundy and Wood model yields a Young's modulus for the site as filled by the substituent impurity ion, rather than the site as occupied by the major constituent species. While this may be meaningful in treating equilibrium partitioning of elements in which the primary consideration is incorporation of the impurity on a specific lattice site, it is not clear that this is the appropriate parameter in the case of diffusion, since ions must travel through the material and occupy intermediate positions en route to specific lattice sites. It seems more likely that the transport properties would in some way reflect the bulk elastic character of the material through which diffusion occurs.

Minerals other than feldspars also show dependence of diffusion rates on cation size and charge. More highly charged cations, including the trivalent REE in zircon (Cherniak et al., 1997a) and diopside (Van Orman et al., 2001) and tetravalent cations in zircon (Cherniak et al., 1997b), exhibit increasing diffusion rates with decreasing ionic radii. Pronounced decreases in diffusivities with higher cation charge have been noted in zircon (Cherniak et al., 1997a,b), clinopyroxene (Sneeringer et al., 1984; Cherniak, 1998a, 2001; Van Orman et al. 1998, 2001), and calcite (Cherniak, 1997, 1998b). Diffusion behavior appears to be correlated with mineral elastic properties, as discussed in Cherniak (1998a). Minerals with larger Young's moduli generally exhibit larger activation energies for diffusion, and consequent lower diffusivities. They also tend to show stronger dependences of diffusion on cation size and charge.

These observations of diffusion behaviors are consistent with a simple elastic model for diffusion (Van Orman et al., 2001). This model, adapted from the work of Mullen (1966) and Zener (1952) assumes that the motion energy of diffusing ions is due to elastic strain and considers the difference in motion energy that results from the difference between the size of an impurity ion and the ideal site radius. This quantity, expressed as a size factor δ, where $\delta = (r_{imp} - r_{site})/r_o$, with r_{imp} the impurity ion radius, r_{site} the ideal site radius, and r_o the average cation-anion distance. The difference between the ideal motion energy E_m^o and that for impurity cations of differing size E_m^i can be expressed as follows:

$$E_m^i = E_m^o\left\{1 + 2\left[\delta\left(1 - 1/\sqrt{2}\right)^{-1} - \delta^2\left(1 - 1/\sqrt{2}\right)^{-2}\right]\right\} \quad (1)$$

Hence, activation energies for diffusion may be greater for cations larger than the ideal size. A relationship relating the diffusivities themselves to ion size can be derived if one assumes that a large proportion of the energy expended in an atomic jump is due to lattice strain. The preexponential factor, D_o, is a function of several parameters, with only motion entropy and jump frequency dependent on the type of diffusing ion rather than the lattice itself. If it is also assumed that differences in jump frequencies among like-charged cations are small, then the log of D_o will be proportional to the motion entropy, S_m, and the motion entropy will be dependent on the temperature derivative of the material's bulk modulus:

$$\ln D_o \propto S_m \approx -\{\partial(\mu/\mu_o)/\partial T\}E_m. \quad (2)$$

Combining these expressions, we then have a relationship between the cation size and diffusion coefficient:

$$\ln D \approx \ln D^{\delta=0} - \frac{2E_m^o}{R}\left[\frac{\partial(\mu/\mu_o)}{\partial T} + \frac{1}{T}\right]\left[\delta\left(1 - 1/\sqrt{2}\right)^{-1} - \delta^2\left(1 - 1/\sqrt{2}\right)^{-2}\right] \quad (3)$$

which can be recast as

$$\ln D \approx \ln D^{\delta=0} - 2b\left[\delta\left(1 - 1/\sqrt{2}\right)^{-1} - \delta^2\left(1 - 1/\sqrt{2}\right)^{-2}\right] \quad (4)$$

This equation describes a parabola with a minimum value when $\delta = 0.146$. For labradorite, the minimum diffusivity will occur for an ionic radius of 0.160 nm; for the less-rigid structure of oligoclase, it will be 0.165 nm. The consistency of the data with this model is evident in Figure 8, where the log of

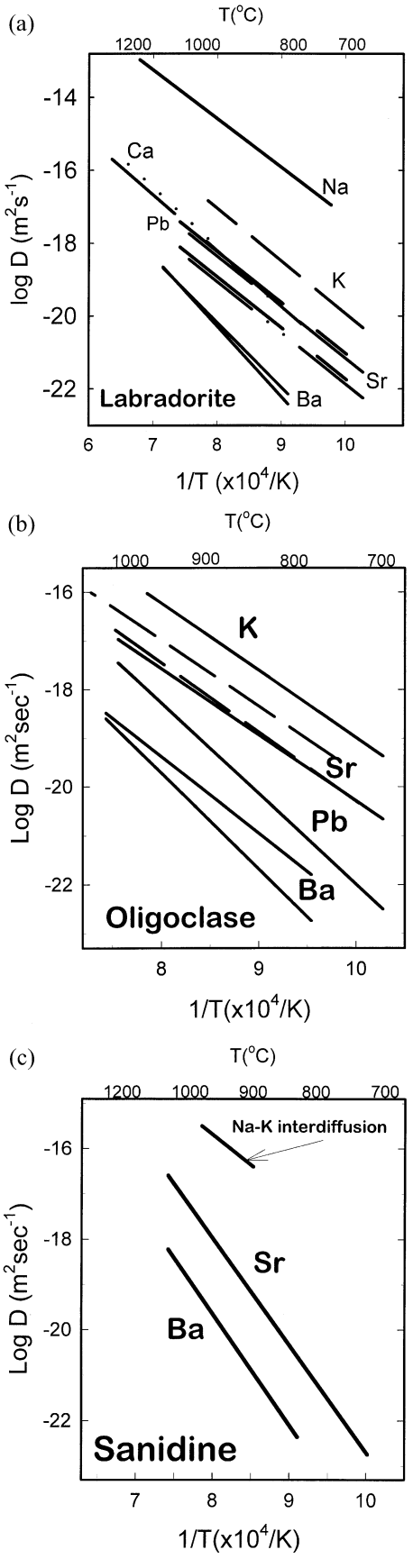

Fig. 7. Summary of cation diffusion data for the three feldspar compositions: (a) labradorite, (b) oligoclase, and (c) sanidine. Sources for data: Ca in labradorite (Behrens et al., 1990), Sr in oligoclase and labradorite (Cherniak and Watson, 1994), Sr in sanidine (Cherniak, 1996), Pb in oligoclase and labradorite (Cherniak, 1995), K in oligoclase and Na and K in labradorite (Giletti and Shanahan, 1997), K-Na interdiffusion in sanidine (Christofferson et al., 1983), and Ba (this study).

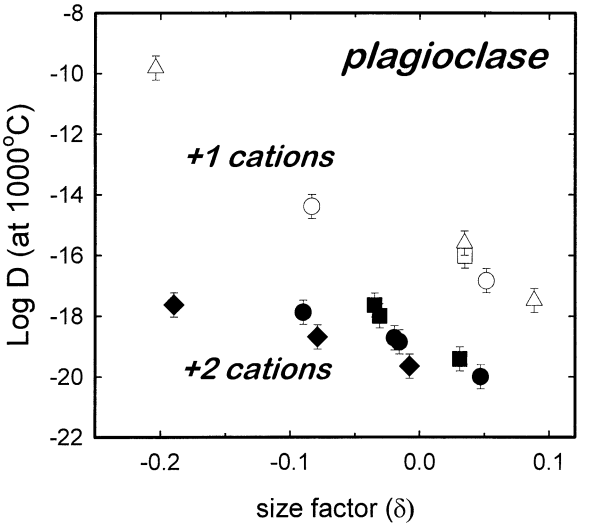

Fig. 8. Plot of Log D at 1000°C vs. the size factor δ for univalent (open symbols) and divalent (filled symbols) cations in plagioclase of various compositions: circles, labradorite; squares, oligoclase; triangles, albite; diamonds, anorthite. The size factor indicates the difference between ideal cation site size and that of an impurity cation substituting on that site, with more negative values for smaller than ideal cations and positive values for larger cations. Size factors are calculated using the mean cation-oxygen bond distances (r_0) for anorthite and albite from Smyth and Bish (1988) and ideal site radii (r_{site}) from Blundy and Wood (1994). Estimates of these radii for intermediate plagioclase compositions are made by weighting the endmember values of r_{site} and r_0, based on their abundance in each plagioclase, which results in values for r_{site} of 0.127 and 0.123 nm for oligoclase and labradorite, respectively, and values for r_0 of 0.258 and 0.255 nm for these feldspar compositions. Increases in D with decreasing size factors are evident for both +1 and +2 cations, which is consistent with an elastic model for diffusion. The extremely fast diffusivity of Li relative to the other univalent cations indicates that, because of its small size, Li may travel interstitially and not substitute on lattice sites in a manner similar to the other alkalis. Sources for data: Behrens et al. (1990), Giletti and Shanahan (1997), La Tourette and Wasserburg (1998), Cherniak and Watson (1994), and Cherniak (1995).

diffusivities of divalent cations in oligoclase and labradorite are plotted as a function of the size factor δ. Also shown are data for other plagioclase compositions and diffusion of univalent cations, which also broadly conform to the trend of increasing *D* with decreasing size factor.

5. Geologic Applications

5.1. Ba Equilibration

The Ba diffusion data reported here permit a determination of the extent to which feldspar grains will equilibrate with their

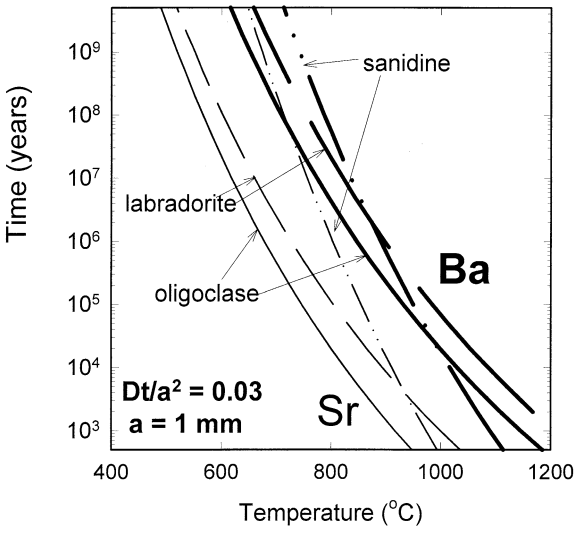

Fig. 9. Preservation of Ba (thick lines) and Sr (finer lines) compositions in feldspar grains subjected to isothermal heating events. Curves represent maximum time-temperature conditions under which grains of 1-mm effective radius will preserve an initial Sr or Ba chemical signature. When conditions above the curves prevail, this information will be lost through diffusional exchange. It will be retained under time-temperature conditions beneath the curves. Calcic plagioclase is more resistant to diffusional alteration than more sodic varieties. Sr compositions or isotope ratios are more likely to be affected by diffusion during thermal events than are Ba chemical signatures.

external environments during a thermal event and potentially alter Ba chemical signatures. We consider a simple model in which the feldspar grains are spheres with radii a and initial uniform Ba concentration of C_1, and are exposed to a medium with concentration C_0. The solution to the diffusion equation at the center of the spheres can then be derived (e.g., Crank, 1975) given these conditions. When the dimensionless parameter Dt/a^2 (where D is the diffusion coefficient and t is the time) is ≤ 0.03, the concentration at the center of the sphere remains unchanged from its initial value. Above 0.03, the concentration at the center of the sphere is affected by the externally imposed concentration C_0 .

In Figure 9 we plot curves representing $Dt/a^2 = 0.03$ for the feldspar compositions investigated in this study. Where anisotropy in diffusion exists, diffusion coefficients for the faster orientation are used in the calculations. An effective diffusion radius of 1mm is used. Also plotted for comparison are curves for Sr equilibration in these feldspars, using the Sr diffusion parameters from Cherniak and Watson (1994) and Cherniak (1996). These curves define the time-temperature limits under which initial Ba (and Sr) compositional information will be retained. For times and temperatures below the curves, Ba concentrations at crystal cores will remain unaffected but will be influenced by the concentration of Ba in the surrounding medium when conditions above the curves exist.

Ba will equilibrate more slowly than Sr in all of the feldspar compositions investigated, given its slower diffusivities. For example, at 800°C, 2-mm diameter sanidine grains will equilibrate with Ba in the surrounding environment in ~50 million yr; Sr in the same sanidine would need only about 1 million yr. At this temperature, plagioclase of comparable size would equilibrate with respect to Ba composition more quickly than the sanidine, i.e., in ~5 million yr for the oligoclase and 20 million yr for labradorite.

5.2. Estimates of Ra Diffusion Coefficients and Implications for ^{226}Ra-^{230}Th Dating

^{226}Ra-^{230}Th dating, by which the disequilibrium between ^{230}Th and its immediate daughter product ^{226}Ra is determined, is used to estimate residence times of young magmas in crustal reservoirs (e.g., Cooper et al., 2001). We can use the relationships between size factor and diffusivities presented in the previous section to estimate the diffusion rates of Ra, and thus determine diffusion timescales for Ra under magmatic conditions. If we fit the labradorite data at 1000°C (Fig. 8) for divalent cations to the parabolic form (Eqn. 4), we obtain values of $\ln D^{\delta=0} = -44.30$ and $b = 4.3$. Given an ionic radius for Ra^{+2} of 0.141 nm (for sixfold coordination, e.g., Shannon, 1976), we obtain a log D of −19.925 and $D = 1.2 \times 10^{-20}$ m^2sec^{-1}. Using an activation energy for diffusion similar to that for Ba (330 kJ mol^{-1}), since Ra and Ba do not differ that greatly in size, we can extrapolate to $D = 1.2 \times 10^{-19}$ m^2sec^{-1} at 1100°C and 3.9×10^{-19} m^2sec^{-1} at 1160°C. Given these diffusivities, Ra diffusion distances in calcic plagioclase grains residing in magma for a few hundred years will be a few tens to ~100 μm and a few to ~10 μm for residence times of a few tens of years, so there is potential for diffusional loss of a significant fraction of Ra in smaller plagioclase grains.

5.3. Preservation of Zoning

Ba has been observed to exhibit significant compositional zoning in feldspar phenocrysts, which can be useful in assessing geochemical evolution in magmatic systems (e.g., Bindeman and Bailey, 1999). It is important, then, to consider under which conditions such zoning may be lost. We consider a simple model with zones of 100 and 10 μm in width. Zones in a feldspar are modeled as plane sheets of thickness l; adjacent planes have different concentrations of diffusant. Only diffusion normal to the planar interface is considered. A (somewhat arbitrary) criterion for alteration of zones is employed. Zones are considered to be "lost" if a compositional change of 10% is attained in the zone's center. The dimensionless parameter Dt/l^2 will be equal to 3.3×10^{-2} when this condition occurs. Figure 10 shows curves constraining the time-temperature conditions under which Ba (and Sr) zoning of these dimensions will be retained in labradorite and sanidine, given the above criteria. In labradorite, for example, 100-μm scale zones would resist obliteration at 700°C for ~50 million yr, with 10-μm zones being preserved for ~500,000 yr. If Sr zoning on the same scale exists, it will be lost more readily; at this temperature 100- and 10-μm Sr zoning will be retained for a few thousand and a few hundred years, respectively. Given the differences in Sr and Ba diffusivities in the feldspar compositions investigated, they should all follow a similar pattern in relative retentivity of zoning. It is clear from these simple calculations that Ba compositional zoning data from feldspars may be among the more robust geochemical indicators of magma evolution.

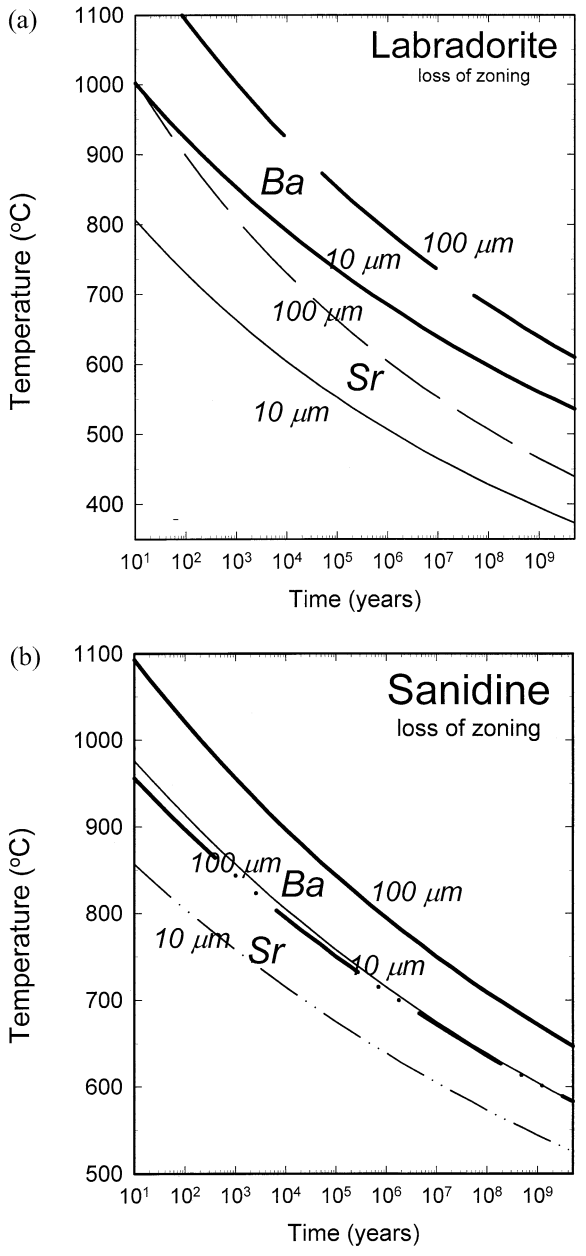

Fig. 10. . Preservation of Ba and Sr zoning in feldspar. Curves (thick lines for Ba, finer lines for Sr) represent maximum time-temperature conditions under which 10- and 100-μm zoning in these elements will be preserved in (a) labradorite and (b) sanidine. For conditions above the curves in each group, well-defined zoning will be lost.

Acknowledgments—I am grateful to Bruce Watson for invaluable discussion and advice throughout the course of this work. Thoughtful comments from Jim Van Orman and an anonymous reviewer helped significantly in improving the manuscript. I thank Dave Wark for assistance with electron microprobe analyses and feldspar orientational advice. Thanks to Paul Pohwat and the Smithsonian's National Museum of Natural History for the labradorite specimen (NMNH # 135512-1). This work was supported by grant EAR-9804794 from the National Science Foundation (to E. B. Watson).

Associate editor: F. J. Ryerson

REFERENCES

Anderson A. T., Davis A. M., and Lu F. (2000) Evolution of Bishop tuff rhyolitic magma based on melt and magnetite inclusions and zoned phenocrysts. *J. Petrol.* **41,** 449–473.

Behrens H., Johannes W., and Schmalzried H. (1990) On the mechanisms of cation diffusion processes in ternary feldspars. *Phys. Chem. Miner.* **17,** 62–78.

Bindeman I. N. and Bailey J. C. (1999) Trace elements in anorthite megacrysts from the Kurile Island Arc: A window to across-arc geochemical variations in magma compositions. *Earth Planet. Sci. Lett.* **169,** 209–226.

Blundy J. D. and Wood B. J. (1991) Crystal-chemical controls on the partitioning of Sr and Ba between plagioclase feldspar, silicate melts, and hydrothermal solutions. *Geochim. Cosmochim. Acta* **55,** 193–210.

Blundy J. and Wood B. (1994) Prediction of crystal-melt partition coefficients from elastic moduli. *Nature* **372,** 452–454.

Cherniak D. J. (1995) Diffusion of lead in plagioclase and K-feldspar: An investigation using Rutherford Backscattering and resonant nuclear reaction analysis. *Contrib. Mineral. Petr.* **120,** 358–371.

Cherniak D. J. (1996) Strontium diffusion in sanidine and albite, and general comments on Sr diffusion in alkali feldspars. *Geochim. Cosmochim. Acta* **60,** 5037–5043.

Cherniak D. J. (1997) An experimental study of Sr and Pb diffusion in calcite, and implications for carbonate diagenesis and metamorphism. *Geochim. Cosmochim. Acta* **61,** 4173–4179.

Cherniak D. J. (1998a) Pb diffusion in clinopyroxene. *Chem. Geol.* **150,** 105–117.

Cherniak D. J. (1998b) REE Diffusion in Calcite. *Earth Planet. Sci. Lett.* **160,** 273–287.

Cherniak D. J. (2001) Pb diffusion in Cr diopside, augite, and enstatite, and consideration of the dependence of cation diffusion in pyroxene on oxygen fugacity. *Chem. Geol.* **177,** 381–397.

Cherniak D. J. and Watson E. B. (1992) A study of strontium diffusion in K-feldspar, Na-K feldspar and anorthite using ion implantation and Rutherford Backscattering spectroscopy. *Earth Planet. Sci. Lett.* **113,** 411–425.

Cherniak D. J. and Watson E. B. (1994) A study of strontium diffusion in plagioclase using Rutherford Backscattering spectroscopy. *Geochim. Cosmochim. Acta* **58,** 5179–5190.

Cherniak D. J., Hanchar J. M., and Watson E. B. (1997a) Rare earth diffusion in zircon. *Chem. Geol.* **134,** 289–301.

Cherniak D. J., Hanchar J. M., and Watson E. B. (1997b) Tetravalent cation diffusion in zircon. *Contrib. Mineral. Petr.* **127,** 383–390.

Christofferson R., Yund, R. A., and Tullis J. (1983) Inter-diffusion of K and Na in alkali feldspars: Diffusion couple experiments. *Am. Mineral.* **68,** 1126–1133.

Cooper K. M., Reid M. R., Murrell M. T., and Clague D. A. (2001) Crystal and magma residence at Kilauea Volcano, Hawaii: ^{230}Th-^{226}Ra dating of the 1955 east rift eruption. *Earth Planet. Sci. Lett.* **184,** 703–718.

Crank J. (1975) *The Mathematics of Diffusion.* 2nd edition, Oxford.

Deer W. A., Howie R. A., and Zussman J. (1992) *An Introduction to the Rock-Forming Minerals.* 2nd edition, Longman, Essex, UK.

Giletti B. J. and Casserly J. E. D. (1994) Sr diffusion kinetics in plagioclase feldspars. *Geochim. Cosmochim. Acta* **58,** 3785–3793.

Giletti B. J. and Shanahan T. M. (1997) Alkali diffusion in plagioclase feldspar. *Chem. Geol.* **139,** 3–20.

Goldsmith J. R. and Jenkins D. M. (1985) The high-low albite relations revealed by reversal of degree of order at high pressures. *Am. Mineral.* **70,** 911–923.

Griffen D. T. (1992) *Silicate Crystal Chemistry.* Oxford.

Grove T. L., Baker M. B., and Kinzler R. J. (1984) Coupled CaAl-NaSi diffusion in plagioclase feldspar: Experiments and applications to cooling rate speedometry. *Geochim. Cosmochim Acta* **48,** 2113–2121.

La Tourette T. and Wasserburg G. J. (1998) Mg diffusion in anorthite: Implications for the formation of early solar system planetesimals. *Earth Planet. Sci. Lett.* **158,** 91–108.

Mullen J. G. (1966) Theory of diffusion in ionic crystals. *Phys. Rev.* **143,** 658–662.

Shannon R. D. (1976) Revised effective ionic radii and systematic

studies of interatomic distances in halides and chalcogenides. *Acta Crystallogr.* **A32,** 751–767.

Singer B. S., Dungan M. A., and Layne G. D. (1995) Textures and Sr, Ba, Mg, Fe, K and Ti compositional profiles in volcanic plagioclase: Clues to the dynamics of calc-alkaline magma chambers. *Am. Mineral.* **80,** 776–798.

Sipling P. J. and Yund R. A. (1974) Kinetics of Al/Si disordering in alkali feldspars, In *Geochemical Transport and Kinetics* (ed. A.W. Hoffman et al.), pp. 185–193, Carnegie Inst. Washington Publ.

Smith J. V. and Brown W. L. (1988) *Feldspar Minerals. Crystal Structures, Physical, Chemical and Microstructural Properties.* Vol. 1, 2nd edition, Springer-Verlag, New York.

Smyth J. R. and Bish D. L. (1988) *Crystal Structures and Cation Sites of the Rock-Forming Minerals.* Allen & Unwin, Boston.

Sneeringer M., Hart S. R., and Shimizu N. (1984) Strontium and samarium diffusion in diopside. *Geochim. Cosmochim. Acta* **48,** 1589–1608.

Van Orman J. A., Grove T. L., and Shimizu N. (1998) Uranium and thorium diffusion in diopside. *Earth Planet. Sci. Lett.* **160,** 505–519.

Van Orman J. A., Grove T. L., and Shimizu N. (2001) Rare earth element diffusion in diopside: Influence of temperature, pressure and ionic radius, and an elastic model for diffusion in silicates. *Contrib. Mineral. Petr.* **141,** 687–703.

Yund R. A. (1983) Diffusion in feldspars. In *Feldspar Mineralogy* (ed. P. H. Ribbe), 2nd ed., pp. 203–222. Mineralogical Society of America, Washington D.C.

Zener C. (1952) Theory of diffusion. In *Imperfections in Nearly Perfect Crystals* (ed. W. Shockley et al.), pp. 289–314, Wiley, New York.